Leveraging organic acids in bipolar membrane electrodialysis (BPMED) can enhance ammonia recovery from scrubber effluents

Mutahi, Gladys; van Lier, Jules B.; Spanjers, Henri

DOI
10.1016/j.watres.2024.122296

Publication date
2024

Document Version
Final published version

Published in
Water Research

Water Research 265 (2024) 122296

Contents lists available at ScienceDirect

Water Research

journal homepage: www.elsevier.com/locate/watres

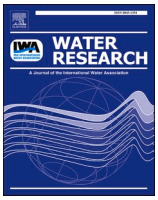

Leveraging organic acids in bipolar membrane electrodialysis (BPMED) can enhance ammonia recovery from scrubber effluents

Gladys Mutahi *, Jules B. van Lier, Henri Spanjers

Delft University of Technology, Department of Water Management, Faculty of Civil Engineering and Geosciences, Stevinweg 1, 2628 CN, Delft, the Netherlands

ARTICLE INFO

Keywords:
Ammonia recovery
Bipolar membrane electrodialysis
Organic acid regeneration
Scrubber effluents
Membrane electrical conductivity
Permselectivity

ABSTRACT

While air stripping combined with acid scrubbing remains a competitive technology for the removal and recovery of ammonia from wastewater streams, its use of strong acids is concerning. Organic acids offer promising alternatives to strong acids like sulphuric acid, but their application remains limited due to high cost. This study proposes an integration of air stripping and organic acid scrubbing with bipolar membrane electrodialysis (BPMED) to regenerate the organic acids. We compared the energy consumption and current efficiency of BPMED in recovering dissolved ammonia and regenerating sulphuric, citric, and maleic acids from synthetic scrubber effluents. Current efficiency was lower when regenerating sulphuric acid (22 %) compared to citric (47 %) and maleic acid (37 %), attributable to the competitive proton transport over ammonium across the cation exchange membrane. Organic salts functioned as buffers, reducing the concentration of free protons, resulting in higher ammonium removal efficiencies with citrate (75 %) and malate (68 %), compared to sulphate (29 %). Consequently, the energy consumption of the BPMED decreased by 54 % and 35 % while regenerating citric and maleic acids, respectively, compared to sulfuric acid. Membrane characterisation experiments showed that the electrical conductivity ranking, ammonium citrate > ammonium malate > ammonium sulphate, was mirrored by the energy consumption (kWh/kg-N recovered) ranking, ammonium sulphate (15.6) < ammonium malate (10.2) < ammonium citrate (7.2), while the permselectivity ranking, ammonium sulphate > ammonium citrate > ammonium malate, aligned with calculated charge densities. This work demonstrates the potential of combining organic acid scrubbers with BPMED for ammonium recovery from wastewater effluents with minimum chemical input.

1. Introduction

Ammonia (NH_3) is an important raw material in the production of nitrogen-based fertilisers essential for food production (Kar et al., 2023; Reis et al., 2016). It is estimated that the Haber Bosch process, used to produce NH_3, consumes approximately 1–2 % of the world's total energy (Qin et al., 2023). An estimated 19 % of the produced NH_3 ends up in the environment emitted from wastewater treatment facilities, agricultural runoff, landfill leachate and industrial liquid waste (Cruz et al., 2019; Deng et al., 2021; Munasinghe-Arachchige and Nirmalakhandan, 2020). Recently, NH_3 has gained research attention as a fuel source and hydrogen carrier in the hydrogen economy, due to its transport flexibility and energy storage capabilities, making it a versatile chemical (El-Shafie and Kambara, 2023; Olabi et al., 2023). Considering its relevance in human sustenance and the subsequent environmental pollution, it is imperative to remove and recover ammonia, to mitigate environmental effects and reduce energy demands.

Municipal wastewaters contain relatively high total ammoniacal nitrogen (TAN) concentrations that have to be reduced before discharging into natural water bodies (Carey and Migliaccio, 2009). As such, advanced regulations to limit TAN discharged from municipal wastewater treatment facilities have been implemented to mitigate environmental impact (Corominas et al., 2013). Recently, the removal and recovery of ammonia from concentrated streams, such as sludge reject water from municipal wastewater treatment plants (WWTP), has been the focus of several studies and reviews (El-Shafie and Kambara, 2023; Mohammadi et al., 2021b; Palakodeti et al., 2021; Ronan et al., 2021; Wu and Vaneeckhaute, 2022; Yellezuome et al., 2022). Conventionally, biological methods involving nitrification and denitrification have been applied to reduce TAN before discharge. However, the aeration requirement makes the technology energy intensive at approximately 45 MJ/kg N removed (Zhang and Liu, 2021). While the

* Corresponding author.
E-mail address: g.mutahi@tudelft.nl (G. Mutahi).

https://doi.org/10.1016/j.watres.2024.122296
Received 4 June 2024; Received in revised form 15 August 2024; Accepted 16 August 2024
Available online 18 August 2024

more recent anaerobic ammonia oxidation (anammox) technology significantly reduces the energy requirement, there are concerns about the emission of N_2O, a potent greenhouse gas, as well as increased sludge production, which in turn increases treatment costs (Cho et al., 2019; Cruz et al., 2019; Dutta et al., 2022). In addition, the presence of *Legionella spp*. in aerosols from full-scale anammox reactors has raised concerns among Dutch water authorities, causing them to hesitate implementing more of these systems (Oesterholt, 2022).

Recent studies indicate that physicochemical methods have great potential in removing and recovering ammonia from wastewater streams without suffering from above constraints (Zhu et al., 2024). These methods include air stripping (Errico et al., 2018; Jamaludin et al., 2018; Kinidi et al., 2018; Vaneeckhaute et al., 2018), adsorption (Fang et al., 2023; Zhao et al., 2023), struvite precipitation (Otieno et al., 2023; Wu and Vaneeckhaute, 2022), capacitive deionisation (Gao et al., 2020; Kurz et al., 2020; Sakar et al., 2017) and membrane based technologies (Gao et al., 2020; Mohammadi et al., 2021b; Saabas and Lee, 2022; Zhu et al., 2024). In particular, ammonia air stripping has been widely applied because it is relatively easy to operate, achieving >90 % ammonia removal from wastewater, and can tolerate solids in the liquid phase (Kar et al., 2023; Kim et al., 2021; Kinidi et al., 2018; Vaneeckhaute et al., 2018). Combining air stripping with acid scrubbing allows for ammonia recovery and reuse as fertiliser, promoting circularity and economic viability (Wu and Vaneeckhaute, 2022).

Air stripping and acid scrubbing, herein referred to as ASAS, is a two-step mass transfer process for ammonia removal and recovery. TAN in wastewater typically exists in two main forms: unionized free ammonia (NH_3) and charged ammonium (NH_4^+). The proportions of these forms depend on the pH of the wastewater (Guštin and Marinšek-Logar, 2011). Sludge reject water from municipal WWTPs typically contain a significant portion of NH_4^+ that is less prone to volatilisation (Eskicioglu et al., 2018; Zhang and Liu, 2021). However, for efficient ammonia removal, the pH of this wastewater is often raised, which increases the proportion of free ammonia (FA) that is more readily transferred to the gas phase during air stripping (Kim et al., 2021). An increased pH is achieved through addition of alkaline agents such as sodium hydroxide (NaOH) or simultaneously stripping of carbon dioxide alongside NH_3 (Campos et al., 2013; Zhao et al., 2015). Increasing temperatures in the range 20–80 °C increase FA by decreasing the solubility of NH_3 in solution. Moreover, increasing airflow rate has shown to influence the interaction between gas and liquid phases by decreasing the boundary layer and consequently enhancing the mass transfer rate from the liquid to the gas phase (Oudad et al., 2022; Walker et al., 2011).

Strong acids such as sulphuric, nitric, hydrochloric acids are used to react with the resulting ammonia-laden air stream, forming ammonium salts. The resulting ammonium salts are considered free from contaminants, including organic compounds and non-volatile substances, due to the selective air stripping process. This allows for direct application of the salts as fertilizers or for processing in various industrial applications, without the need for purification. (Kinidi et al., 2018; Palakodeti et al., 2021; Yellezuome et al., 2022). Nonetheless, to obtain high purity fertilisers, supplying excess acid is critical, necessitating the storage of significant amounts of acids at ASAS facilities (Hadlocon et al., 2014; Jamaludin et al., 2018).

Most ASAS processes reported in literature utilize sulphuric acid (H_2SO_4) to completely protonate ammonia due to its comparatively low price and the extensive market for the resulting $(NH_4)_2SO_4$ (van Zelm et al., 2020; Vaneeckhaute et al., 2017). The use of strong acids poses operational and safety concerns due to their corrosive nature and potential health hazards to operators, prompting the need for research into safer acid alternatives (Soto-Herranz et al., 2022; Yellezuome et al., 2022). While Ashtari et al. (2016) proposed the use of dilute H_2SO_4 (up to pH 4) in acid scrubbers to protonate ammonia in waste air streams, this approach necessitates modifications to the scrubber operation, including reduced flow velocities and increased acid dosages, which may lead to additional operational expenses (Ashtari et al., 2016).

While there is relatively limited research on the use of organic acids as scrubbing agents in ASAS installations, existing studies have demonstrated their potential as alternatives to sulfuric acid. A comparative study by Jamaludin et al. (2018) demonstrated that citric acid has scrubbing efficiencies comparable to sulfuric acid (Jamaludin et al., 2018). Additionally, a theoretical study by Starmans and Melse (2011) highlighted the feasibility of citric and maleic acids, considering factors such as ammonia binding strength, biodegradability of the resulting liquid fertilizer, and safety during handling (Starmans and Melse, 2011). Another study, conducted by Soto-Herranz et al. (2022), evaluated eight scrubbing solutions for ammonia removal using a gas permeable membrane. From an environmental, economic, and capture efficiency standpoint, water, phosphoric acid, and citric acid emerged as viable alternatives to sulfuric acid (Soto-Herranz et al., 2022). Despite their promising potential, the implementation of organic acids as scrubbing agents at pilot scale and full-scale ASAS installations is yet to be demonstrated. This can be attributed to the higher cost of organic acids compared to sulfuric acid and the absence of a commercial market for the resulting ammonium salts due to regulatory challenges (Jamaludin et al., 2018).

To mitigate the costs associated with organic acids, coupling a bipolar membrane electrodialysis (BPMED) unit downstream of the ASAS process presents a promising solution. BPMED combines the salt-separation functions of conventional electrodialysis with the water-dissociation functions of bipolar membranes (Pärnamäe et al., 2021). A BPMED unit consists of ion exchange membranes that transport charged ions from one side of the membrane to the other, under the influence of an electric field. Positively charged ions (cations) are transported across the cation exchange membrane (CEM), while negatively charged ions (anions) are transported across the anion exchange membrane (AEM). The addition of bipolar membranes (BPM) facilitates the dissociation of water into hydroxyl ions (OH^-) and protons (H^+), enabling the formation of base and acid streams from the cation and anion stream respectively (Bak et al., 2019).

In recent years, BPMED has emerged as a promising technology for recovering ammonium from various wastewater streams on laboratory scale (Li et al., 2021; Mohammadi et al., 2021a; Rodrigues et al., 2020; van Linden et al., 2020), and pilot scale (Ferrari et al., 2022; Ward et al., 2018). Wastewater containing ammonium is introduced into a BPMED stack, where ammonium ions migrate towards the base compartment through the CEM while anions are collected in the acid compartment. Within the base compartment, ammonium ions react with OH− to form dissolved ammonia ($NH_3.H_2O/NH_4OH$), while in the acid compartment, a mixture of anions and the addition of H^+ leads to the formation of an acidic stream (Shi et al., 2020). Wastewaters often contain various cations that may be transported together with ammonium across the CEM, resulting in an impure base stream and a decrease in the process's current efficiency. In addition, the membranes used in BPMED processes are susceptible to fouling and scaling induced by the presence of organic compounds and divalent cations in the wastewaters (Ferrari et al., 2022). This membrane degradation not only reduces ammonia recovery efficiency but also increases energy consumption and operational expenses due to the need for frequent membrane cleaning (Shi et al., 2018, 2020). Moreover, in most of these studies, the acidic stream generated during the process is often overlooked, whose disposal poses significant environmental and safety concerns due to its high acidity and other contaminants.

The proposed combination of ASAS and BPMED offers several advantages. First, the upstream ASAS process eliminates non-volatile organic compounds and divalent cations from the wastewater stream through selective ammonia removal, thereby protecting the ion exchange membranes in the BPMED from fouling and scaling. This could potentially extend the lifespan of the membranes and reduce the operational costs associated with frequent cleaning and membrane replacement. Furthermore, the acid stream regenerated during the BPMED process can be directly recycled in the ASAS process and used as

scrubbing agent, minimising the need for additional chemical inputs, reducing the overall cost of the ASAS process. Finally, the recovered dissolved NH_3 can be used for purposes beyond conventional fertiliser production. NH_3 is a versatile chemical with a wide range of applications such as hydrogen carrier, production of industrial solvents and urea (Olabi et al., 2023).

Ammonium effluents generated from ASAS processes exhibit varying pH, temperature, and concentration, differentiating them from wastewater streams investigated in BPMED studies, such as reject water, urine, and pig manure hydrolysate (Gao et al., 2020; Rodrigues et al., 2020; Shi et al., 2018, 2020; van Linden et al., 2020). The treatment of ASAS process effluents using BPMED has not yet been investigated. While Saabas and Lee (2022) successfully recovered ammonia from a simulated membrane contactor effluent using BPMED, the study assumed an initial ammonium sulphate concentration of 2 g-N/l (Saabas and Lee, 2022). This concentration may not accurately reflect higher ammonium concentrations typically associated with ASAS effluents (Kinidi et al., 2018). Moreover, the experiments were done using a strong acid (sulphuric acid) as a draw solution to recover ammonia from wastewater in the upstream process.

Scrubber effluents from ASAS processes using organic acids contain organic acid anions. This presents a unique challenge in their regeneration in the subsequent BPMED process because ion exchange membranes are in contact with organic electrolytes. The separation and transport mechanisms of organic electrolytes differ significantly from those of inorganic electrolytes. Inorganic electrolytes are primarily separated based on steric effects, whereas organic electrolytes are influenced by multiple factors, including ionization constant, molecular size, and the structure of the organic ions (Chandra et al., 2022; Jörissen et al., 2003; Melnikov et al., 2018). Moreover, past studies have drawn attention to the interaction between organic anions and the fixed charge of ion exchange membranes, effectively decreasing membrane resistance (Chandra et al., 2019, 2022; Chandra et al., 2018; Jörissen et al., 2003). Therefore, investigating the impact of organic acid anions on ammonium ion transport during the BPMED process is crucial for optimizing energy consumption. To the best of our knowledge, the regeneration of organic acids from scrubber effluents containing ammonium and organic acid anions has not been reported.

This study compared for the first time the influence of acid anion on the recovery of ammonium from simulated scrubber effluents, using BPMED configured with bipolar membranes and cation exchange membranes (BP-C). We used three salts—ammonium sulphate, ammonium citrate and ammonium malate—to recover dissolved NH_3 while regenerating the respective acids. We compared the BPMED performance based on energy consumption, recovery efficiency and current efficiency, under constant current conditions. Furthermore, to elucidate the influence of electrolytes on current efficiency, we investigated the behaviour of the cation exchange membrane when exposed to the different electrolytes. To this end, we characterised the electrical conductivity and permselectivity of the membranes used and examined their correlation to energy consumption. By demonstrating a 52 % reduction in BPMED energy consumption, our study highlights the potential of integrating organic acid scrubbers with BPMED technology. This approach not only minimises the chemical inputs during scrubbing process but also creates a more energy efficient treatment train for ammonium wastewaters.

2. Materials and methods

2.1. Experimental setup

Fig. 1 shows a schematic representation of the experimental setup used in this work. An electrodialysis laboratory unit ED 64004 (PCCell GmbH, Heusweiler, Germany) was used. It consisted of a Pt/Ir-MMO coated and Ti-stretched anode and a stainless-steel cathode both with electrode area of 8 cm × 8 cm and placed in a polypropylene electrode housing material. Between the cathode and anode, a membrane stack consisting of ten cell pairs was placed. Each cell pair consisted of a PC SK

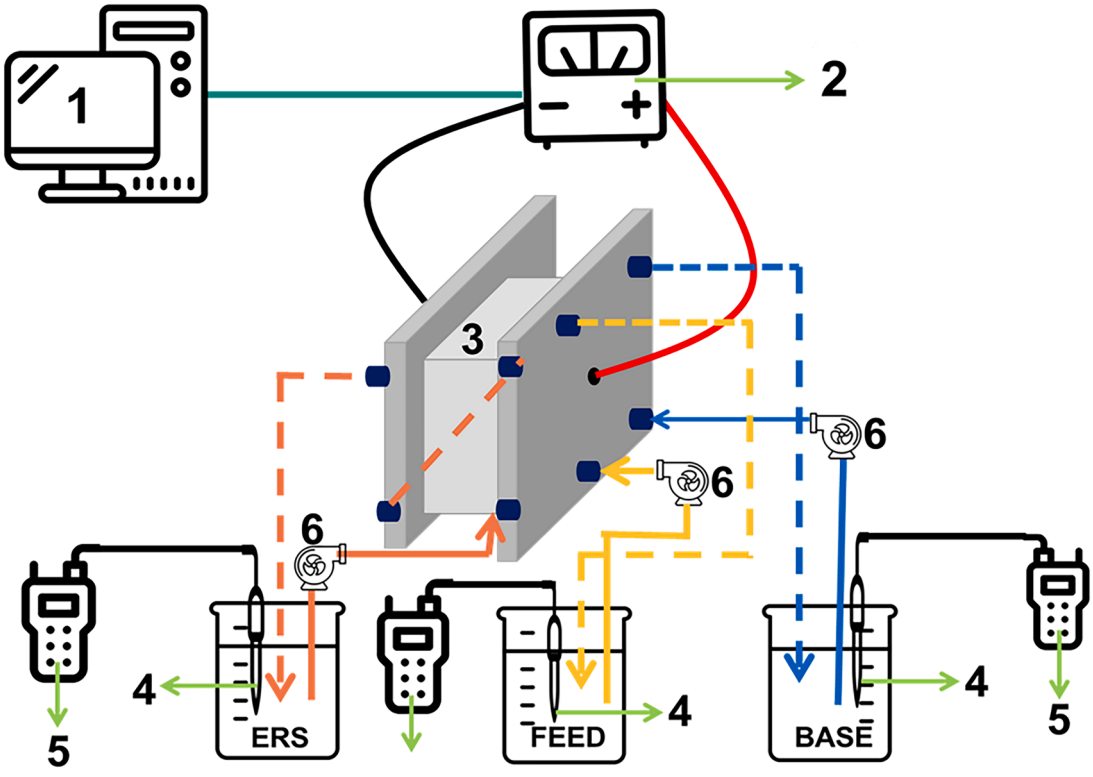

Fig. 1. Schematic representation of the experimental set up including workstation (1), power supply unit (2), the BPMED membrane stack (3), pH and electrical conductivity probes (4), multi-meters (5) and pumps (6).

cation exchange membrane (CEM) and PC bip bipolar membrane (BPM) arranged alternatingly to form a two compartment BPMED arrangement (BP-C) as shown in Fig. 2. The membranes had an effective area of 8 cm × 8 cm per membrane. Feed and base compartments were formed by separating adjacent membranes by polypropylene spacers (PCCell) with a thickness of 0.45 mm and porosity of 59 %. To prevent mixing of the electrode solution with the feed and base solutions, two PC MTE cation end exchange membranes (CEEMs) were positioned adjacent to the electrode compartments (van Linden et al., 2019). The properties of the used membranes obtained from the manufacturer are listed in Table 1. A DC power supply unit (Voltcraft, Germany) with voltage range (0–36 V) and current range (0–10 A) was used to supply electric current between the electrodes.

The feed, base and electrode rinsing solutions were stored in 2 L double jacketed, thermostable glass cylinders, connected in circuits with magnetically coupled centrifugal pumps (ITS-Betzel, Germany), which allowed the recirculation of solutions inside the membrane stack. The feed and base circuits were equipped with flow-through meters (10–100 L/h) to measure the flow rate through the stack (ASV Stubbe, Germany), pre-filters, pressure measurement devices, and membrane valves to control the flow through the stack. The flow rate through the stack was controlled by adjusting the membrane valves until the desired flow rate (30 L/h), corresponding to a membrane crossflow velocity of 3.6 cm/s was achieved. The flow rate through the electrode compartments was set to 75 L/h.

2.2. Chemical reagents

The feed solutions were prepared to mimic the characteristics of scrubber effluents generated from ASAS processes, employed for treating reject water (initially containing up to 2 g-N/l), produced during sludge dewatering in municipal WWTPs. Scrubber effluents from ASAS using sulfuric acid typically comprise ammonium sulphate and residual sulfuric acid (Ukwuani and Tao, 2016). In our study, we assumed a three-factor increase in nitrogen concentration of reject water after the implementation of ASAS, resulting in a scrubber effluent with a nitrogen concentration of 6 g-N/l. While the pH of such effluents vary between 2 and 8 (Kinidi et al., 2018), no pH adjustment was done on the initial pH of solutions in our study.

The synthetic salt solutions were prepared by dissolving a specific amount of ammonium salt used in this study (ammonium citrate (≥97 %, Carl Roth GmbH, Germany) and ammonium sulphate (Sigma-Aldrich, Germany) in 1.5 L demi water, corresponding to an initial concentration of 6 g-N/l. Ammonium malate was prepared by dissolving 72 % ammonia solution (Sigma-Aldrich, Germany) in demi water to achieve a 6 g-N/l solution. Maleic acid was added to the prepared solution until pH 6 was reached for ammonium malate (National Center for Biotechnology Information, 2024).

The initial solutions in the base compartment were prepared by dissolving 1 g of the respective salts in 1 L of demi water to increase conductivity at the start of each test and to lower overall stack resistance (van Linden et al., 2020). In all experiments, the electrode rinsing solution was prepared by dissolving 71 g of sodium sulphate (>99 % Sigma-Aldrich, Germany) to produce a 0.5 M solution (Saabas and Lee, 2022).

2.3. Methods

2.3.1. BPMED experiment

An electrodialysis stack composed of bipolar membranes (BPM) and cation exchange membranes (CEM) was used in this study, creating a BP-C cell arrangement. Ammonium salts were introduced into the compartment between the BPM and CEM, where under the influence of an electric field, NH_4^+ ions migrated through the CEM. These ions combined with OH^- ions generated by the BPM located on the opposite side of the CEM, resulting into the formation of ammonium hydroxide (NH_4OH). In the feed solution, the transported NH_4^+ were replaced with H^+ ions generated by the BPM, regenerating the acid as the acid anions remained in the feed solution.

For a focused investigation of ammonium transport, a BP-C

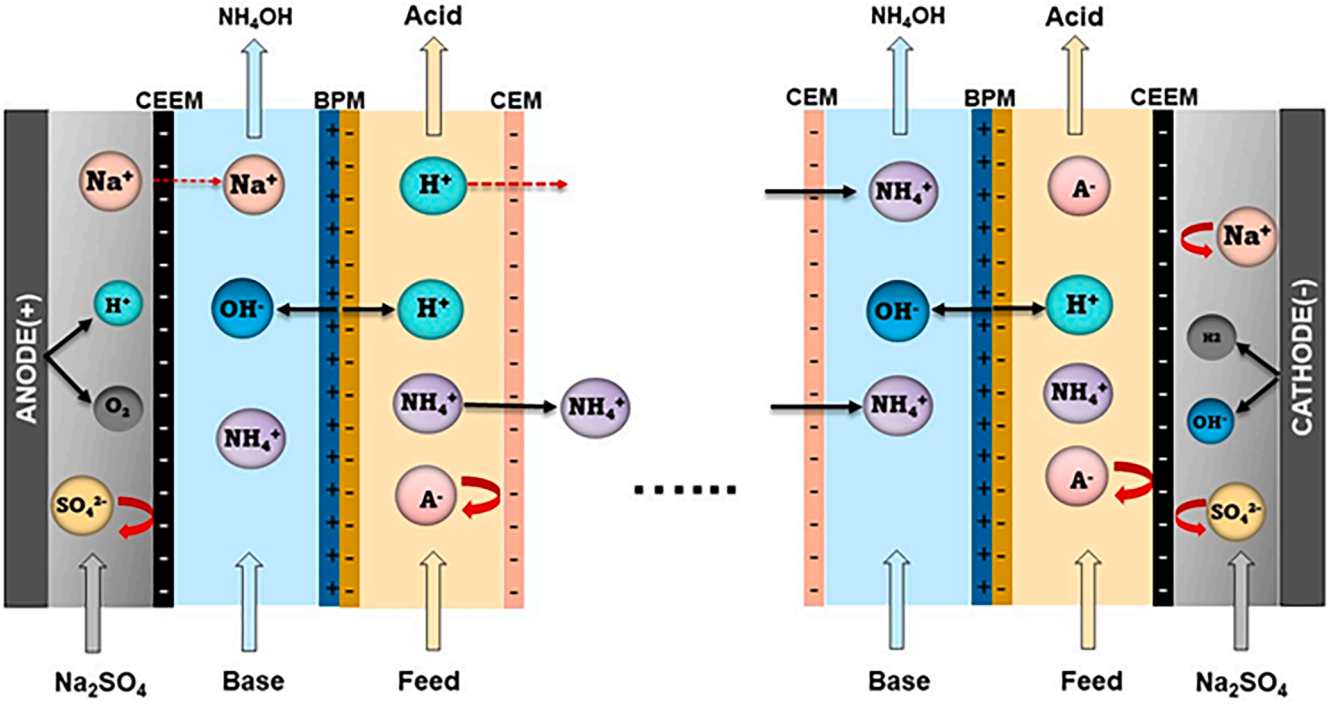

Fig. 2. Schematic representation of the flow of ions inside the BPMED membrane stack. Simulated scrubber effluent was introduced in the feed compartment. Under an applied electric current, NH_4^+ ions were transported to the base compartment through the CEM, where they reacted with OH^- ions generated by the BPM to form dissolved NH_3. In the feed compartment, the acid anions were retained and due to addition of H^+, acid was regenerated.

Table 1
Properties of membranes used in this study. Data obtained from technical datasheet provided by PCCell GmbH, Heusweiler, Germany.

Membrane	Thickness (μm)	Ion exchange capacity(meq g^{-1})	Water content (wt. %)	Transport number (KCl (0.1/ 0.5 N)	Area resistance specific (Ω cm^2)	Water dissociation efficiency
PC-SK	100–120	3	9	>95 %	2.5	–
PC MTE	220	1.8	–	>94 %	4.5	–
PC-bip	200–350	–	–	–	–	>95 % at 0.8–1 V/BPM

arrangement was selected. This configuration minimises transport of acid anions, mitigating possible current inefficiencies. Such a scenario would not be achievable in a BP-A arrangement, consisting of BPM and anion exchange membranes (AEM). Moreover, BP-C cell arrangement allowed the investigation of the effect of proton transport on current efficiency. This is because protons produced by the BPM could potentially compete with ammonium as current carriers across the CEM. While stacking both CEM and AEMs in a (BP-C-A) cell arrangement could achieve the objective of evaluating proton competition, stacking membranes in this manner would introduce additional electrical resistance as well as generate a dilute waste stream (He et al., 2023; Rodrigues et al., 2020).

Tests were conducted for each ammonium salt, in batch mode at an initial room temperature of 25 ± 2 °C. Prior to each test, the tanks were emptied of the liquids from the previous tests, and demi water was circulated over the BPMED stack until a solution conductivity below 100 μS/cm and neutral pH (6–7) was reached in all tanks. The tanks were filled with fresh demi water if the pH and conductivities were not at the desired values after several minutes of operation.

An electrodialysis unit control application (PCCell frontend software) developed by PCCell GmbH, Heusweiler, Germany, was used to control the power supply unit and to monitor voltage and current, recorded every 2 s in a csv file. Prior to activating the power supply on the PC frontend software, the solutions were recirculated over the BPMED stack for at least five minutes to ensure complete mixing and to allow air bubbles to escape. Afterwards, the experiment was started by initiating power supply on the PC frontend software. Each batch test was conducted in a constant current mode at 156 A/m^2, which corresponded to the limiting current density (LCD) determined using Cowan and Brown LCD method (Cowan and Brown, 1959). The batches were run for 2 h, to ensure an equal supply of charge for all tests. Samples for analysis were collected from the recirculating solutions at the beginning of each test and subsequently every 30 min. The experiments were conducted in duplicates and the results presented in this study are the average values obtained from independent runs.

2.3.2. Membrane characterization

2.3.2.1. Resistance and conductivity. A series of additional experiments were conducted to obtain current-voltage curves to calculate the resistance and conductivity of the used cation exchange membranes when exposed to electrolytes used in this study i.e. ammonium sulphate, citrate, and malate. Membrane resistance measurements have been used to indicate interactions between electrolytes and membranes (Barros et al., 2021; Huang et al., 2022; Zhu et al., 2018). The area specific resistances (ASR) of the used CEMs membranes were measured in different electrolyte solutions at equimolar concentrations using a six-compartment electrochemical setup with a four-electrode configuration (Redstack BV, The Netherlands), following a procedure described by (Barros et al., 2021). Fig. 3 illustrates the resistance measurement setup.

A CEM previously used in our BPMED experiments with an active membrane area of 9.6 cm^2 (3.5 cm diameter circle) was placed in between two compartments of the cell (compartment 3 and 4) containing electrolyte test solution. Prior to each measurement, the membrane was equilibrated with the test solution for at least 24 h. On either sides of the test compartments, buffer compartments (compartment 2 and 5) were filled with buffer solutions to minimize the influence of electrode reactions on the working electrodes (Balster et al., 2007). On each side of the buffer compartments, the electrode compartments (compartment 1 and 6) with electrodes were used as the working and counter electrode. Two double junction Ag/AgCl reference electrodes placed on either side of the test membrane were used to measure the electrical potential of the

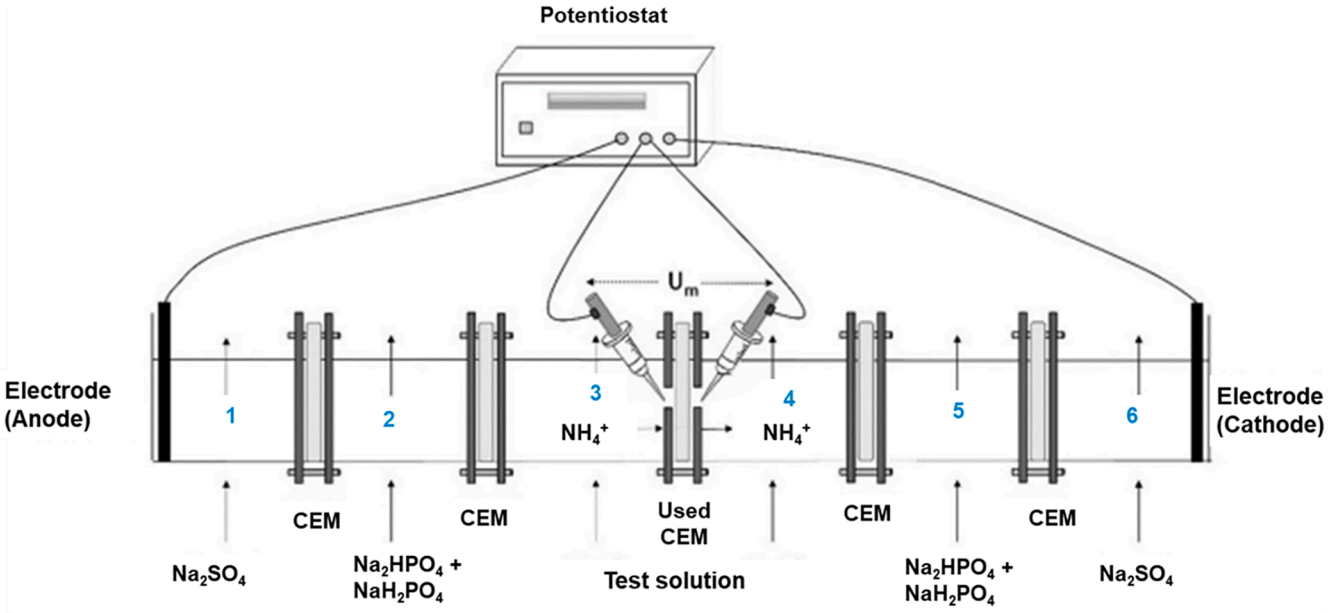

Fig. 3. A schematic diagram of the six-compartment cell used to measure the area specific resistances of the used cation exchange membrane. Diagram adapted from ref (Barros et al., 2021) and modified to fit this study.

membrane. One molar equivalent (eq) of test solutions (ammonium sulphate, ammonium citrate, and ammonium malate), buffer solutions (1 eq Na_2HPO_4. NaH_2PO_4) and electrode rinsing (1 eq Na_2SO4) solutions were circulated at 170 mL/min (Chinello et al., 2024) using a peristaltic pump to reduce the effects of concentration polarisation. A stepwise direct current was applied to the electrodes from 1 to 8 mA in increments of 1 mA using Autolab PGSTAT 128 N potentiostat (Metrohm, Switzerland). The applied current and potential difference between the reference electrode and the working electrode were recorded in the workstation every second. The combined resistance of the membrane and the test solution was derived from the slope of the voltage as a function of applied current. The same procedure was repeated but without the membrane in place, to measure the resistance of the solution. To obtain the ASR of the membrane, the solution resistance was subtracted from the combined resistance. For each test electrolyte solution, duplicate ASR were obtained from the same membrane. The thickness of the membrane was obtained from the manufacturer (Table 1) and the electrical conductivity of the membrane calculated from the ASR (in Ω cm^2) using Eq. (1).

$$k = \frac{l}{ASR} \tag{1}$$

Where k is the electrical conductivity of the membrane (mS/cm) and l is the membrane thickness (cm).

2.3.2.2. Permselectivity measurements. Permselectivity describes an ion exchange membrane's preference for transporting ions with an opposite charge (counterions) compared to ions with the same charge (co-ions), and is related to the transport number of ions (Długołęcki et al., 2008). Permselectivity arises from the interaction between ions and membrane's fixed charge: co-ions are repelled while counterions are attracted (Luo et al., 2018). Exclusion of co-ions is controlled by Donnan potential, an electrical potential difference developed at the solution-membrane interface. However, counterion interaction with the membrane reduces the membranes fixed charge density, weakening the Donnan exclusion effect, consequently decreasing permselectivity (Huang et al., 2022).

Permselectivity measurements could further elucidate the effect of electrolyte on the selectivity of the CEM in transporting NH_4^+ ions when exposed to different co-ion identities such as citrate, malate, and sulphate. A static permselectivity procedure was followed using a two-compartment set-up as described by (Petrov et al., 2023). In this method, a potential arises across the membrane when in contact with the same electrolyte of unequal concentration.

CEM previously used in our BPMED experiments with an active membrane area of 9.6 cm^2 (3.5 cm diameter circle) was placed in between the two chambers of the cell. On either side of the membrane, the compartments were filled with the same electrolyte but different concentrations, maintaining a ratio of 5, that is: C high/ C low = 5, where C high and C low are the high and low concentrations, respectively. The high concentrations used were identical to the initial concentration applied in the BPMED experiments. Prior to each test, the membranes were equilibrated in the high concentration solution for at least 24 h. The solutions were recirculated at 40 mL/min to minimise the effects of concentration polarisation. Two double junction Ag/AgCl reference electrodes connected to Autolab PGSTAT 128 N potentiostat (Metrohm, Switzerland), were used to measure the potential difference developed across the CEM. The potential was recorded on the workstation every second in open circuit voltage mode for thirty minutes to ensure equilibration. Permselectivity was calculated from i) the measured membrane potential, ii) theoretical (Nernst) potential, iii) ion transport numbers in the membrane and solution phases for each of the three electrolytes, and iv) activity coefficients of the high and low solutions. Equations are provided in the supplementary material (Eqs. (S1)–(S10)).

2.4. Analytical methods

Ammonium concentrations were measured using ion chromatography, Metrohm Compact IC Flex 930 (Metrohm Nederland, Schiedam, The Netherlands). Electrical conductivity and pH of all solutions were measured every minute, in their respective tanks using calibrated TetraCon 925 EC-sensors and IDS SenTix 940 pH sensors from Xylem Analytics, Germany. The measurements were recorded in WTW Multi 3630 IDS multimeters (Xylem Analytics, Germany).

2.5. Data analysis of the BPMED experiment

To assess the efficiency of the BPMED unit for ammonium recovery, the ratio of the amount of ammonium accumulated in the base to the total ammonium transported from the feed was calculated as:

$$\eta NH_4^+ t\ (\%) = \frac{mNH_4^+ bt}{mNH_4^+ f0} \times 100\ \% \tag{2}$$

where $mNH_4^+ f0$ (g) refers to the amount of ammonium in the feed at time = 0 and $mNH_4^+ bt$ (g) the amount accumulated in the base compartments after time t (t is the total experiment run time).

Current efficiency (CE, %) and energy consumption (E, kWh/ kg-N) are key indicators that describe the performance of BPMED units (Guo et al., 2023; van Linden et al., 2020).

CE is the ratio of the charge used to transport ammonium ions to the total supplied charge, expressed as:

$$CE = \frac{z \times F \times nNH_4^+}{N \times \sum_0^t (I_{\Delta t} \times \Delta t)} \tag{3}$$

where z is the ions' valence ($z = 1$ for NH_4^+), F is Faraday constant (96,485 C/mol). nNH_4^+(mol) is the amount of ammonium accumulated in the base after time t, N is the number of cell pairs ($N = 10$), $I_{\Delta t}$ is the average current (in A) applied during each time interval and Δt is the time interval (in s).

E (kWh/kg N), based on recovered ammonium was calculated using the following equation:

$$E = \frac{\sum_0^t (U_{\Delta t} \times I_{\Delta t} \times \Delta t)}{3600 \times mNH_4^+, b} \tag{4}$$

where $U_{\Delta t}$ = average voltage (in V) of membrane stack at each time and mNH_4^+(in g-N) is the amount of ammonium recovered in the base after time t.

3. Results and discussions

3.1. Variations in solutions' electrical conductivity did not influence overall stack resistance

Solutions containing anions of weak organic acids exist in a dynamic equilibrium between charged anions and neutral acid molecules, with the relative proportions of each form depending on the pH of the salt solutions (Chandra et al., 2019, 2022). In this study, the initial pH of the ammonium salt solutions was selected to ensure that the ammonium salts were fully dissociated into their constituent ions, namely NH_4^+ and organic acid anions. Under an electric field, the NH_4^+ ions were transported from the feed solution to the base solution via the cation exchange membrane (CEM). Fig. 4a depicts the electrical conductivity of the feed solutions over time. Despite equal initial nitrogen concentrations (Fig. 4b), ammonium sulphate solution (AmS) exhibited a higher initial electrical conductivity (EC) compared to the organic salt solutions of ammonium citrate (AmC) and ammonium malate (AmM). As a strong electrolyte, AmS completely deionises in solution, while AmC and AmM retain some fraction of neutral organic acid molecules that do not contribute to EC. As NH_4^+ ions in the acid stream were transported

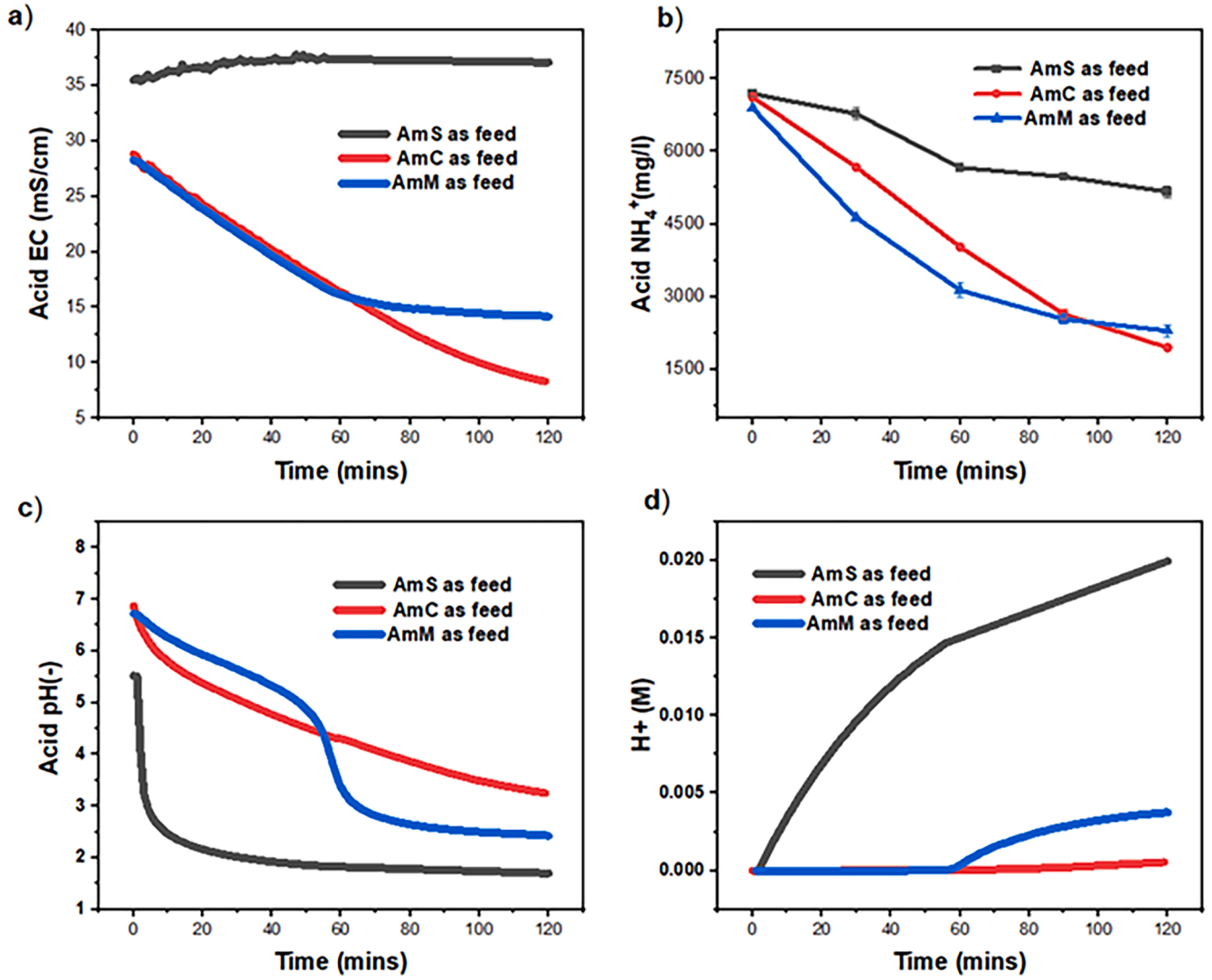

Fig. 4. Change in a) acid electrical conductivity, b) acid NH_4^+ concentration, c) acid pH and d) H^+ concentration over time for sulphate, citrate, and malate salts during bipolar membrane electrodialysis. Applied current was 156 A/m^2 and experimental period lasted 2 h, using bipolar membrane and cation exchange membrane (BP-C) arrangement. Mean values from duplicate experiments are presented, with error bars indicating the minimum and maximum values observed.

towards the base stream, the EC of the organic solutions gradually decreased. H^+ ions generated by the BPM to replace the transported NH_4^+ led to a decrease in pH (Fig. 4c), which shifted the equilibrium towards the formation of less conductive neutral acid molecules. Following an hour of operation, the EC of the AmM feed solution remained stable. Moreover, the pH of the AmM feed solution reached a steady state of less than 3. Under this pH condition, molecular maleic acid dominated as the main species in the solution (He et al., 2023). In contrast to AmC and AmM, the electrical conductivity of AmS solution remained constant throughout the two-hour experiment. The reaction between protons generated by the bipolar membrane (BPM) and sulphate counterions led to the formation of sulphuric acid (H_2SO_4). Being a strong acid, the dissociation of H_2SO_4 yielded highly conductive H^+ ions into the solution, effectively compensating for the loss of NH_4^+ ions and maintaining a constant EC value.

The EC of feed solutions influences the electric potential drop across the membrane stack in an electrodialysis process. A higher EC corresponds to lower overall stack resistances, indicating greater ionic mobility and reduced energy consumption (Tanaka, 2015; Yan et al., 2019). However, although variations in EC were observed among the tested solutions, the corresponding changes in voltage drop and stack resistances (Fig. S1), remained within the margin of error, indicating that the EC variations did not corelate with stack resistance.

3.2. *Ammonium recovery efficiency was higher for ammonium citrate and ammonium malate solutions compared to ammonium sulphate solution*

Fig. 5a depicts the ammonium concentration in the base stream over time. NH_4^+ concentration increased over time for all feed solutions. After 2 h of experiment, we calculated the ammonium recovery efficiency using Eq. (2), which followed the order citrate (60.1 ± 0.1 %) > malate (49.6 ± 0.5 %) > sulphate (27.8 ± 0.7 %). Compared to similar NH_4^+ recovery studies (Saabas and Lee, 2022; van Linden et al., 2020), the ammonium recovery efficiencies obtained for in this study were lower, which can be attributed to methodological differences. We calculate recovery efficiency based on NH_4^+ accumulated in the base solution (Eq. (2)), whereas cited studies use total NH_4^+ transported, neglecting potential losses. This difference likely explains the lower values observed in this study. Furthermore, direct comparisons were challenging due to the absence of research on NH_4^+ recovery from organic salts using BPMED.

To explain the differences between the recovery efficiencies amongst the tested salts, we examined the pH of the feed solution during the experiments. On the one hand, the pH of ammonium sulphate (AmS)

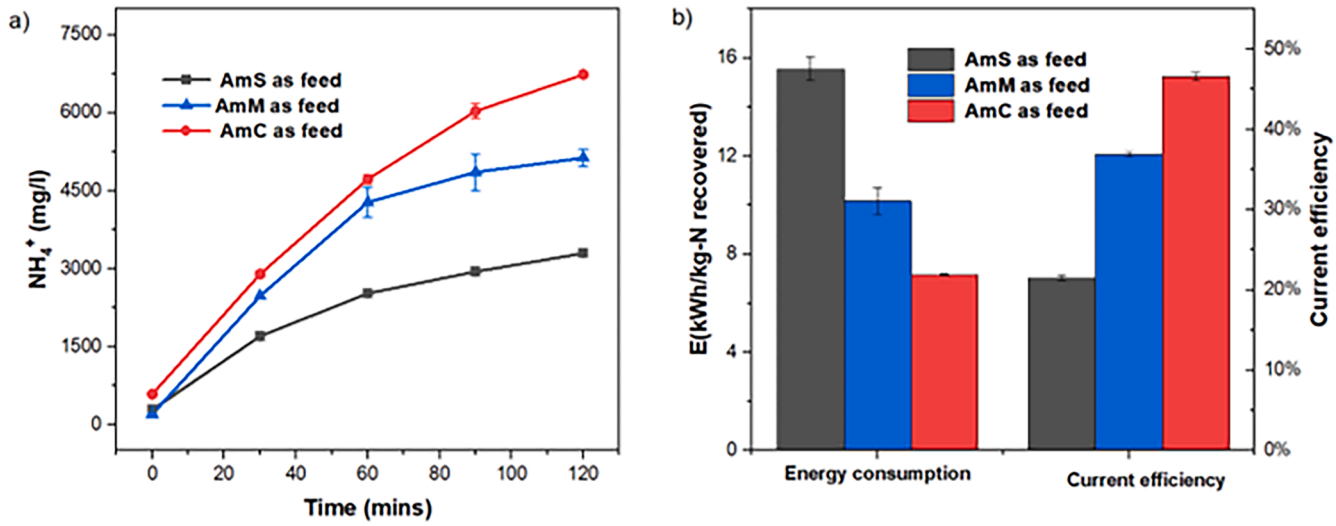

Fig. 5. a) NH_4^+ concentration in the base over time for sulphate, citrate, and malate salts during bipolar membrane electrodialysis. b) energy consumption and current efficiency. Applied current was 156 A/m^2 and experimental period lasted 2 h, using bipolar membrane and cation exchange membrane (BP-C) arrangement. Mean values from duplicate experiments are presented, with error bars indicating the minimum and maximum values.

feed solution decreased from pH 5.5 to pH 2 within the initial five minutes as shown in Fig. 4c, corresponding to an increased concentration of free protons (Fig. 4d). On the other hand, the pH of the organic salts decreased gradually as a function of time, like the EC behaviour observed in Fig. 4a. Consequently, free proton concentration, calculated from the pH, was higher in AmS feed solution compared to AmC and AmM solutions. At low pH, a competition between NH_4^+ and H^+ for transport across the cation-exchange membrane was created and because H^+ has a higher mobility and a smaller hydration radius compared to NH_4^+ (Luo et al., 2018), H^+ would be preferentially transported across the CEM, explaining the lower recovery efficiencies observed for ammonium sulphate solution.

However, as salts of weak carboxylic acids with different pKa values (Chandra et al., 2019), AmC and AmM functioned as buffers, enabling their conjugate bases (Cit^{3-} and Mal^{2-}) to neutralize the H^+ ions generated by the BPM, decreasing the free H^+ concentration in the feed solution. This reduced free proton concentration minimized the competition with NH_4^+ ions for transport, facilitating higher ammonium recovery from these solutions. The differences in recovery efficiencies observed for citrate and malate is discussed in Section 3.4.

3.3. Free proton concentrations in the feed solutions influence current efficiency and energy consumption

The current efficiency was lower when the BPMED was operated using the AmS solution (21.5 ± 0.3) % compared to when operated using AmM (36.9 ± 0.9 %) and AmC (46.5 ± 0.5 %) feed solutions, shown in Fig. 5b. The loss of current can be attributed to H^+ transport over the CEM, as the free proton concentration was higher for AmS solution. Consequently, twice the energy consumption was required to transport NH_4^+ from the AmS feed solution than to transport it from the AmC feed solution.

Additionally, higher pH values in the base stream promotes the conversion of NH_4^+ to nonconductive NH_3 gas according to

$$NH_4^+ + OH^- \rightleftharpoons NH_3 + H_2O,\ pKa = 9.25, \quad (5)$$

potentially increasing base compartment resistance and energy consumption. However, observed variations in base conductivity (Supplementary information, Fig. S1d), did not appear to impact overall stack resistances (Supplementary information, Fig. S1b), suggesting minimal influence of base conductivity on energy consumption in our setup.

Although the energy consumptions (7–15 kWh/kg-N recovered) obtained in this study were comparable to the conventional Haber Bosch process, the highest current efficiency obtained was lower than efficiencies in similar studies involving ammonium recovery (Guo et al., 2021; Rodrigues et al., 2020; van Linden et al., 2020). Loss in current can be attributed to undesired processes such as co-ion leakage due to poor membrane selectivity, competitive transport of H^+, electro-osmosis, and membrane fouling/scaling (Chandra et al., 2018; Rodrigues et al., 2023). Additionally, neutral NH_3 molecules in the base compartment (Eq. (5)), could diffuse through the ion exchange membranes to adjacent compartments. When the NH_3 diffuses into the feed compartment where the pH is low (Fig. 4c), it converts back to NH_4^+.This back-and-forward transport of NH_4^+ ions, known as back diffusion, causes the same NH_4^+ to be transported multiple times though the CEM, reducing current efficiency (Rodrigues et al., 2023; van Linden et al., 2020).

In this study, foulant free feed solutions were used, minimising membrane fouling. Moreover, these feed solutions did not contain divalent cations that increase the risk of membrane scaling. While the pH of the base streams during our experiments was always above 9.3 (see supplementary information Fig. S1(c)), in the two-hour experiment, NH_3 back diffusion and repetitive transport was negligible since the concentration of NH_4^+ in the base (Fig. 5a) did not seem to plateau. Nevertheless, the current loss resulting from the diffusion of NH_3 towards the electrode compartment was always below 7 % across all experiments (see supplementary information for calculation details). Therefore, with ammonia diffusion, membrane fouling and scaling excluded, we suspected competitive transport of H^+ across the CEM as the mechanism responsible for the observed current loss.

To evaluate the extent of current loss resulting from H^+ competition, experiments were conducted using an alkaline buffer system. We assessed the energy consumption (kWh/kg-N recovered) and current efficiency (%) of the BPMED process with synthetic solution containing ammonium bicarbonate (AmB) as the feed solution. While carbonic acid exhibits low scrubbing efficiencies during ammonia removal from waste air streams (Soto-Herranz et al., 2022), bicarbonate is a dominant ammonium counterion in real reject water streams (van Linden et al., 2019).

Fig. 6 shows the performance of the AmB feed stream compared to the AmC feed stream. The feed stream of the bicarbonate counter-ion exhibited negligible free proton concentrations. As a result, a 16.8 ± 2.3 % improvement in current efficiency was observed while energy consumption decreased by 8.3 ± 1.6 %.

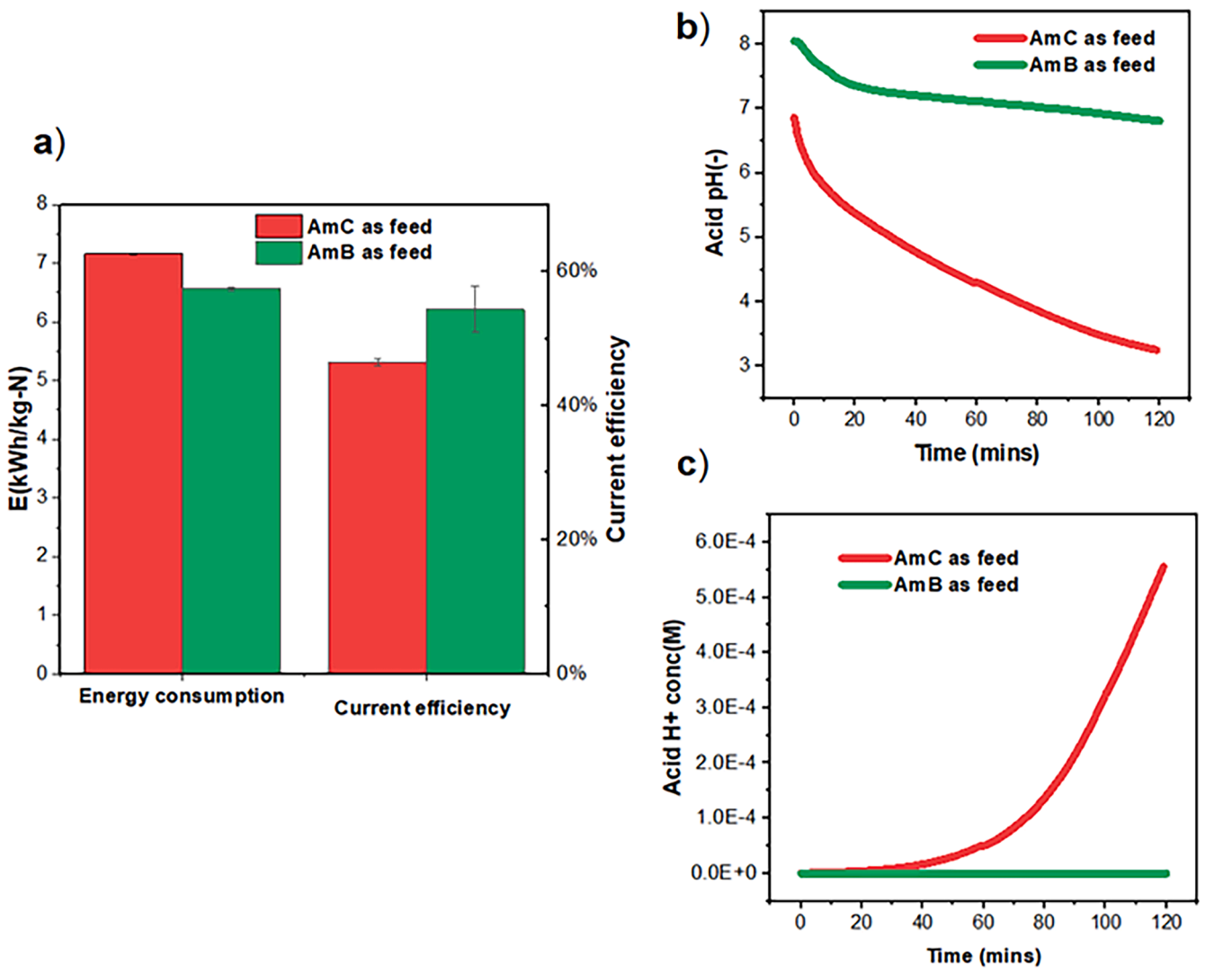

Fig. 6. a) A comparison of energy consumption and current efficiency between ammonium citrate and ammonium bicarbonate salts b) course of pH and c) H^+ concentration in the feed over time, during bipolar membrane electrodialysis. Applied current was 156 A/m^2 and experimental period lasted 2 h, using bipolar membrane and cation exchange membrane (BP-C) arrangement. Mean values from duplicate experiments are presented, with error bars indicating the minimum and maximum values observed.

Despite minimizing the free proton concentration in the AmB feed solution, the current efficiency remained below 70 %. This observation suggested that mitigating proton competition, while important, was not the exclusive mechanism by which the organic acids enhanced NH_4^+ recovery during the BPMED process. Although the same membrane material was used in all experiments, we hypothesized that the presence of varying anions might have influenced the membranes' selectivity. While literature reports interactions between organic anions and anion exchange membranes during the production of organic acids (Chandra et al., 2019), such interactions with the CEMs have not been reported before. Additional experiments were conducted as described in the materials and methods Section 2.3.2, to characterise the electrical conductivity and permselectivity of the membrane in varying electrolytes.

3.4. *Electrical conductivity of the used cation exchange membrane was sensitive to co-ion identity*

Membrane resistance contributes to the total resistance experienced by ions during their transport in an electrodialysis system. It is a function of operating conditions, particularly the composition and concentration of electrolytes (Barros et al., 2021). A higher conductivity, corresponding to a lower membrane resistance, is desirable in electrodialysis as it translates to lower energy consumption. We calculated the conductivities of the used CEMs in electrolytes with different anions (SO_4^{2-}, Cit^{3-} and Mal^{2-}) identity but equal NH_4^+ concentration using Eq. (1).

Our results showed that for electrolytes with the same cation (NH_4^+) the anion identity influenced the membrane conductivity. As shown in Fig. 7, the membrane conductivity was highest when in contact with AmC (10.3 ± 0.5 mS/cm) followed by AmM (7.7 ± 0.3 mS/cm) and AmS (6.3 ± 0.6 mS/cm). Consequently, the BPMED energy consumption trend mirrored the obtained membrane conductivity pattern, with AmC requiring the least energy (7.16 ± 0.04 kWh/kg-N recovered) followed by AmM (10.16 ± 0.56 kWh/kg-N recovered) and AmS (15.55 ± 0.49 kWh/kg-N recovered). Research directly comparing the influence of inorganic and organic electrolytes on membrane conductivity is limited. While Huang et al. (2022) observed minimal influence of anion type on CEM conductivity using inorganic salt solutions (sodium sulphate, sodium chloride and sodium bromide), their study focused on inorganic anions (Huang et al., 2022). Our observations regarding the differences in membrane conductivities of CEM exposed to AmC and AmM align with (Melnikov et al., 2018). The authors report an increasing CEM

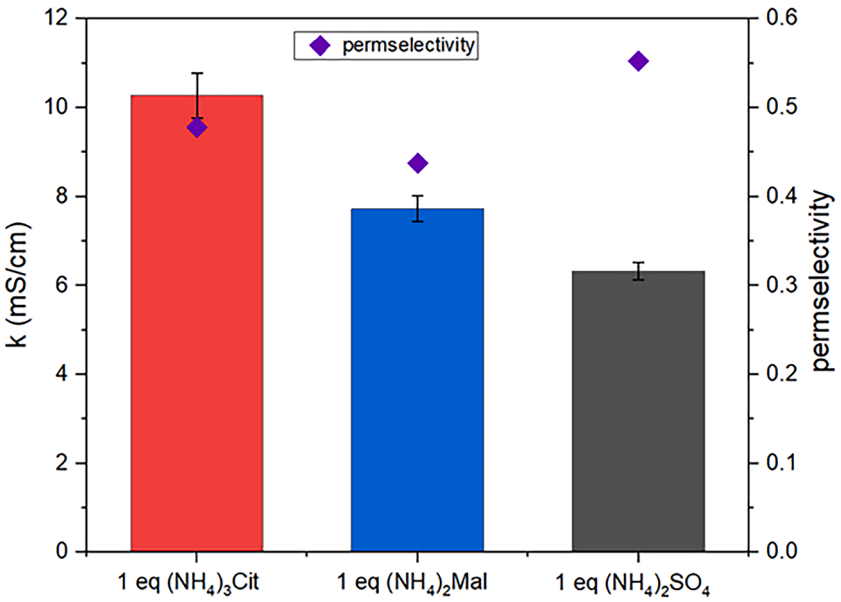

Fig. 7. Measured cation exchange membrane conductivities (bars) and permselectivity (diamonds) when in contact with solutions of molar equivalents concentrations of ammonium citrate (AmC), ammonium malate (AmM) and ammonium sulphate (AmS). Mean values from duplicate experiments are presented, with error bars indicating the minimum and maximum values observed.

conductivity with mono-, di- and tri- basic organic acids in the order of citric > succinic > acetic. They attribute this trend to the varying lengths of carboxylic acid chain within the anions, potentially influencing their interactions with the membrane's fixed charge (Melnikov et al., 2018). Our results suggest a similar possible influence of the carboxylic chain length on NH_4^+ transport mechanisms but this requires further investigations.

3.5. Anion identity influenced the permselectivity of the CEM but did not explain the energy consumption trend observed

The permselectivity of the used membranes in electrolytes AmS, AmC and AmM was calculated following the static potential measurement method and using Eqs. (S2)–(S18). The initial pH of these electrolytes matched the initial pH of the feed solutions used in the BPMED experiments (Fig. 4c). NH_4^+ transport in the CEM was driven by a concentration gradient where it would diffuse from the high concentration side to the low concentration side. Diffusion is primarily influenced by the stokes radius of the counterion (NH_4^+), solution composition and ion's affinity over the CEM (Chandra et al., 2019). Since the same CEM in the same concentration of counterion (NH_4^+) was used, we anticipated equal membrane permselectivity. However, the composition of solutions with varying co-ions (present with NH_4^+), seemed to play a role in determining the membrane permselectivity. Fig. 7 shows that the membrane permselectivity followed the order AmS > AmC > AmM. Epsztein et al. demonstrated that smaller ions with higher charge densities experience greater Donnan exclusion by charged nanofiltration membranes compared to larger ions (Epsztein et al., 2018). Therefore, the charge densities of the co-ions were calculated using the following equation:

$$\text{Charge density} = \frac{ze}{(4/3)\pi r^3}. \tag{6}$$

where z is the charge of ion ($z(NH_4^+) = 1$, $z(SO_4^{2-}) = -2$, $z(Cit^{3-}) = -3$, and $z(Mal^{2-}) = -2$), e is the elementary charge (1.6×10^{-19} C), and r is the stokes (hydrated) ionic radius (Å). The calculated charge densities in mC/cm^3 were SO_4^{2-} (6.28) > Mal^{2-} (3.84) > Cit^{3-} (2.92), corresponding to increasing stokes radius (Å), SO_4^{2-} (2.3) < Mal^{2-} (2.7) < Cit^{3-} (3.4) (Luo et al., 2018). Our findings align with theoretical predictions that SO_4^{2-} with its higher charge density would experience a stronger Donnan exclusion within the CEM and consequently increase the permselectivity towards NH_4^+. However, an opposite permselectivity behaviour was followed for organic anions. It appears that for organic anions, charge densities alone were insufficient in explaining the observed permselectivity behaviour and that perhaps other factors such as electrolyte pH play a role in influencing their interaction with a CEM membrane as demonstrated by (Chandra et al., 2022) for anion exchange membranes.

The observed permselectivity behaviours did not directly translate to the energy consumption values obtained from BPMED experiments. This likely indicates the presence of counteracting effects. For example, the competition between H^+ and NH_4^+ for transport at lower pH could possibly counteract the positive effect of high SO_4^{2-} charge density for AmS. A lower pH, indicating a higher free proton concentration (Fig. 4c and d), appears to have decreased the membrane selectivity for NH_4^+. This could have resulted in the lower ammonium recovery efficiency and higher energy consumption observed. Further investigations that include permselectivity measurements in electrolytes with lower pH to verify this hypothesis are necessary.

4. Conclusions

This study demonstrated simultaneous dissolved ammonia recovery and acid regeneration from three different salts (ammonium sulphate, ammonium citrate, and ammonium malate) with an initial concentration of 6 g-N/l, through a bipolar membrane electrodialysis process. Without using additional chemicals, acids (sulphuric, citric, and maleic acid) with final pH values of 1.7, 3.3 and 2.4, respectively, were regenerated from their respective salts. Organic electrolytes appeared to function as buffers, limiting pH changes during the BPMED process. This buffering effect likely contributed to the higher ammonium removal and current efficiency observed for ammonium citrate and ammonium malate solutions compared to ammonium sulphate solution, which consistently exhibited lower pH values. Ammonium sulphate solution exhibited the highest energy consumption followed by ammonium malate and ammonium citrate. Besides the variations in free protons concentrations, differences in membrane electrical conductivity could explain the observed energy consumption trend, with ammonium citrate displaying the highest conductivity followed by ammonium malate and

ammonium sulphate. However, additional mathematical modelling is necessary to improve the understanding of the interaction between organic anions and cation exchange membranes. The substitution of sulphuric acid with citric acid in recovering ammonia in air stripping and acid scrubbing technologies is likely to result in a 54 ± 3 % decrease in energy consumption of the subsequent BPMED process when regenerating the acid. While the synthetic scrubber effluents used in this study mimicked real scrubbing effluents, verification studies with real scrubber effluents are necessary for scaling up purposes.

CRediT authorship contribution statement

Gladys Mutahi: Writing – original draft, Visualization, Validation, Methodology, Investigation, Formal analysis, Data curation, Conceptualization. **Jules B. van Lier:** Writing – review & editing, Supervision, Project administration. **Henri Spanjers:** Writing – review & editing, Supervision, Project administration.

Declaration of competing interest

The authors declare the following financial interests/personal relationships which may be considered as potential competing interests:

Gladys Mutahi reports financial support was provided by Netherlands Enterprise Agency. If there are other authors, they declare that they have no known competing financial interests or personal relationships that could have appeared to influence the work reported in this paper.

Data availability

Data will be made available on request.

Acknowledgements

This work was supported by the Netherlands Enterprise Agency, also known as 'Rijksdienst voor Ondernemend Nederland' (RVO) [Project no. TEHE119005]. This study was performed within the "Kostprijsreductie bioenergie door Chemical Free Ammonium Recovery" (NoChemNAR) research. The authors would like to acknowledge Tuur van den Eijnde and Ian Tomassen from Nijhuis Saur Industries for reviewing the final draft.

Supplementary materials

Supplementary material associated with this article can be found, in the online version, at doi:10.1016/j.watres.2024.122296.

References

Ashtari, A.K., Majd, A.M.S., Riskowski, G.L., Mukhtar, S., Zhao, L., 2016. Removing ammonia from air with a constant pH, slightly acidic water spray wet scrubber using recycled scrubbing solution. Front. Environ. Sci. Eng. 10 (6) https://doi.org/10.1007/s11783-016-0869-3.

Bak, C., Yun, Y.M., Kim, J.H., Kang, S., 2019. Electrodialytic separation of volatile fatty acids from hydrogen fermented food wastes. Int. J. Hydrogen Energy 44 (6), 3356–3362. https://doi.org/10.1016/J.IJHYDENE.2018.07.134.

Balster, J., Yildirim, M.H., Stamatialis, D.F., Ibanez, R., Lammertink, R.G.H., Jordan, V., Wessling, M., 2007. Morphology and microtopology of cation-exchange polymers and the origin of the overlimiting current. J. Phys. Chem B 111 (9), 2152–2165. https://doi.org/10.1021/jp068474t.

Barros, K.S., Martí-Calatayud, M.C., Scarazzato, T., Bernardes, A.M., Espinosa, D.C.R., Pérez-Herranz, V., 2021. Investigation of ion-exchange membranes by means of chronopotentiometry: a comprehensive review on this highly informative and multipurpose technique. Adv. Colloid Interface Sci. 293, 102439 https://doi.org/10.1016/j.cis.2021.102439.

Campos, J.C., Moura, D., Costa, A.P., Yokoyama, L., Araujo, F.V.d.F., Cammarota, M.C., Cardillo, L., 2013. Evaluation of pH, alkalinity and temperature during air stripping process for ammonia removal from landfill leachate. J. Environ. Sci. Health, Part A 48 (9), 1105–1113.

Carey, R.O., Migliaccio, K.W., 2009. Contribution of wastewater treatment plant effluents to nutrient dynamics in aquatic systems: a review. Environ. Manag. 44, 205–217.

Chandra, A., E, B., Chattopadhyay, S, 2019. Physicochemical interactions of organic acids influencing microstructure and permselectivity of anion exchange membrane. Colloids Surf. A 560, 260–269. https://doi.org/10.1016/j.colsurfa.2018.10.029.

Chandra, A., E, B., Chattopadhyay, S, 2022. A critical analysis on ion transport of organic acid mixture through an anion-exchange membrane during electrodialysis. Chem. Eng. Res. Des. 178, 13–24. https://doi.org/10.1016/j.cherd.2021.11.035.

Chandra, A., Tadimeti, J.G.D., Chattopadhyay, S., 2018. Transport hindrances with electrodialytic recovery of citric acid from solution of strong electrolytes. Chin. J. Chem. Eng. 26 (2), 278–292. https://doi.org/10.1016/j.cjche.2017.05.010.

Chinello, D., Post, J., de Smet, L.C.P.M., 2024. Selective separation of nitrate from chloride using PVDF-based anion-exchange membranes. Desalination 572, 117084. https://doi.org/10.1016/j.desal.2023.117084.

Cho, S., Kambey, C., Nguyen, V.K., 2019. Performance of anammox processes for wastewater treatment: a critical review on effects of operational conditions and environmental stresses. Water 12 (1), 20.

Corominas, L., Acuña, V., Ginebreda, A., Poch, M., 2013. Integration of freshwater environmental policies and wastewater treatment plant management. Sci. Total Environ. 445–446, 185–191. https://doi.org/10.1016/j.scitotenv.2012.12.055.

Cowan, D.A., Brown, J.H., 1959. Effect of turbulence on limiting current in electrodialysis cells. Ind. Eng. Chem. 51 (12), 1445–1448.

Cruz, H., Law, Y.Y., Guest, J.S., Rabaey, K., Batstone, D., Laycock, B., Verstraete, W., Pikaar, I., 2019. Mainstream ammonium recovery to advance sustainable urban wastewater management. Environ. Sci. Technol. 53 (19), 11066–11079.

Deng, Z., van Linden, N., Guillen, E., Spanjers, H., van Lier, J.B., 2021. Recovery and applications of ammoniacal nitrogen from nitrogen-loaded residual streams: a review. J. Environ. Manag. 295, 113096 https://doi.org/10.1016/j.jenvman.2021.113096.

Długołęcki, P., Nymeijer, K., Metz, S., Wessling, M., 2008. Current status of ion exchange membranes for power generation from salinity gradients. J. Memb. Sci. 319 (1), 214–222. https://doi.org/10.1016/j.memsci.2008.03.037.

Dutta, A., Kalam, S., Lee, J., 2022. Elucidating the inherent fouling tolerance of membrane contactors for ammonia recovery from wastewater. J. Memb. Sci. 645, 120197 https://doi.org/10.1016/j.memsci.2021.120197.

El-Shafie, M., Kambara, S., 2023. Recent advances in ammonia synthesis technologies: toward future zero carbon emissions. Int. J. Hydrogen Energy 48 (30), 11237–11273. https://doi.org/10.1016/j.ijhydene.2022.09.061.

Epsztein, R., Shaulsky, E., Dizge, N., Warsinger, D.M., Elimelech, M., 2018. Role of ionic charge density in donnan exclusion of monovalent anions by nanofiltration. Environ. Sci. Technol. 52 (7), 4108–4116. https://doi.org/10.1021/acs.est.7b06400.

Errico, M., Fjerbaek Sotoft, L., Kjærhuus Nielsen, A., Norddahl, B., 2018. Treatment costs of ammonia recovery from biogas digestate by air stripping analyzed by process simulation. Clean. Technol. Environ. Policy 20 (7), 1479–1489. https://doi.org/10.1007/s10098-017-1468-0.

Eskicioglu, C., Galvagno, G., Cimon, C., 2018. Approaches and processes for ammonia removal from side-streams of municipal effluent treatment plants. Bioresour. Technol. 268, 797–810. https://doi.org/10.1016/j.biortech.2018.07.020.

Fang, S., Li, G., Shi, H., Ye, J., Wang, H., Ding, X., Luo, L., Li, G., Yang, M., 2023. Preparation of low-cost functionalized diatomite and its effective removal of ammonia nitrogen from wastewater. Environ. Sci. Pollut. Res. 30 (44), 98881–98894.

Ferrari, F., Pijuan, M., Molenaar, S., Duinslaeger, N., Sleutels, T., Kuntke, P., Radjenovic, J., 2022. Ammonia recovery from anaerobic digester centrate using onsite pilot scale bipolar membrane electrodialysis coupled to membrane stripping. Water Res. 218, 118504 https://doi.org/10.1016/j.watres.2022.118504.

Gao, F., Wang, L., Wang, J., Zhang, H., Lin, S., 2020. Nutrient recovery from treated wastewater by a hybrid electrochemical sequence integrating bipolar membrane electrodialysis and membrane capacitive deionization. Environ. Sci. 6 (2), 383–391. https://doi.org/10.1039/c9ew00981g.

Guo, H., Yuan, P., Pavlovic, V., Barber, J., Kim, Y., 2021. Ammonium sulfate production from wastewater and low-grade sulfuric acid using bipolar- and cation-exchange membranes. J. Clean. Prod. 285 https://doi.org/10.1016/j.jclepro.2020.124888.

Guo, X., Chen, J., Wang, X., Li, Y., Liu, Y., Jiang, B., 2023. Sustainable ammonia recovery from low strength wastewater by the integrated ion exchange and bipolar membrane electrodialysis with membrane contactor system. In: Sep. Purif. Technol., 305 https://doi.org/10.1016/j.seppur.2022.122429.

Guštin, S., Marinšek-Logar, R., 2011. Effect of pH, temperature and air flow rate on the continuous ammonia stripping of the anaerobic digestion effluent. Process Saf. Environ. Prot. 89 (1), 61–66. https://doi.org/10.1016/j.psep.2010.11.001.

Hadlocon, L.J., Lingying, W.Z., Roderick, M., 2014. Optimization of ammonia absorption using acid spray wet scrubbers. Trans. ASABE, pp. 647–659. https://doi.org/10.13031/trans.57.10481.

He, J., Zhou, R., Dong, Z., Yan, J., Ma, X., Liu, W., Sun, L., Li, C., Yan, H., Wang, Y., Xu, T., 2023. Bipolar membrane electrodialysis for cleaner production of diprotic malic acid: separation mechanism and performance evaluation. Membranes (Basel) 13 (2). https://doi.org/10.3390/membranes13020197.

Huang, Y., Fan, H., Yip, N., 2022. Influence of electrolyte on concentration-induced conductivity-permselectivity tradeoff of ion-exchange membranes. J. Memb. Sci. 668, 121184 https://doi.org/10.1016/j.memsci.2022.121184.

Jamaludin, Z., Rollings-Scattergood, S., Lutes, K., Vaneeckhaute, C., 2018. Evaluation of sustainable scrubbing agents for ammonia recovery from anaerobic digestate. Bioresour. Technol. 270, 596–602. https://doi.org/10.1016/j.biortech.2018.09.007.

Jörissen, J., Breiter, S.M., Funk, C., 2003. Ion transport in anion exchange membranes in presence of multivalent anions like sulfate or phosphate. J. Memb. Sci. 213 (1–2), 247–261.
Kar, S., Singh, R., Gurian, P.L., Hendricks, A., Kohl, P., McKelvey, S., Spatari, S., 2023. Life cycle assessment and techno-economic analysis of nitrogen recovery by ammonia air-stripping from wastewater treatment. Sci. Total Environ. 857, 159499 https://doi.org/10.1016/j.scitotenv.2022.159499.
Kim, E.J., Kim, H., Lee, E., 2021. Influence of ammonia stripping parameters on the efficiency and mass transfer rate of ammonia removal. Appl. Sci. 11 (1), 441. https://doi.org/10.3390/app11010441.
Kinidi, L., Tan, I.A.W., Abdul Wahab, N.B., Tamrin, K.F.B., Hipolito, C.N., Salleh, S.F, 2018. Recent development in ammonia stripping process for industrial wastewater treatment. In: International Journal of Chemical Engineering, 2018. Hindawi Limited.
Kurz, E.E.C., Hellriegel, U., Luong, V.T., Bundschuh, J., Hoinkis, J., 2020. Selective ion adsorption with pilot-scale membrane capacitive deionization (Mcdi): arsenic, ammonium, and manganese removal. Desalin. Water Treat. 198, 163–169. https://doi.org/10.5004/dwt.2020.26036.
Li, Y., Wang, R., Shi, S., Cao, H., Yip, N.Y., Lin, S., 2021. Bipolar membrane electrodialysis for ammonia recovery from synthetic urine: experiments, modeling, and performance analysis. Environ. Sci. Technol. 55 (21), 14886–14896. https://doi.org/10.1021/acs.est.1c05316.
Luo, T., Abdu, S., Wessling, M., 2018. Selectivity of ion exchange membranes: a review. J. Memb. Sci. 555, 429–454. https://doi.org/10.1016/j.memsci.2018.03.051.
Melnikov, S., Kolot, D., Nosova, E., Zabolotskiy, V., 2018. Peculiarities of transport-structural parameters of ion-exchange membranes in solutions containing anions of carboxylic acids. J. Memb. Sci. 557, 1–12. https://doi.org/10.1016/j.memsci.2018.04.017.
Mohammadi, M., Guo, H., Yuan, P., Pavlovic, V., Barber, J., Kim, Y., 2021a. Ammonia separation from wastewater using bipolar membrane electrodialysis. Electrochem. Sci. Adv. https://doi.org/10.1002/elsa.202000030.
Mohammadi, R., Tang, W., Sillanpää, M., 2021b. A systematic review and statistical analysis of nutrient recovery from municipal wastewater by electrodialysis. In: Desalination, 498. Elsevier B.V.
Munasinghe-Arachchige, S.P., Nirmalakhandan, N., 2020. Nitrogen-fertilizer recovery from the centrate of anaerobically digested sludge. Environ. Sci. Technol. Lett. 7 (7), 450–459. https://doi.org/10.1021/acs.estlett.0c00355.
National Center for Biotechnology Information, 2024. PubChem Compound Summary For CID 13644148, Ammonium malate. Retrieved January 08 from. https://pubchem.ncbi.nlm.nih.gov/compound/Ammonium-malate.
Oesterholt, F., 2022. First Edition of Guide for Legionella Prevention in Biological Wastewater Treatment Plants is Made Public. K. W. Research. https://www.kwrwater.nl/en/actueel/first-edition-of-guide-for-legionella-prevention-in-biological-wastewater-treatment-plants-is-made-public/.
Olabi, A.G., Abdelkareem, M.A., Al-Murisi, M., Shehata, N., Alami, A.H., Radwan, A., Wilberforce, T., Chae, K.-J., Sayed, E.T., 2023. Recent progress in green ammonia: production, applications, assessment; barriers, and its role in achieving the sustainable development goals. Energy Convers. Manag. 277, 116594 https://doi.org/10.1016/j.enconman.2022.116594.
Otieno, B., Funani, C.K., Khune, S.M., Kabuba, J., Osifo, P., 2023. Struvite recovery from anaerobically digested waste-activated sludge: a short review. J. Mater. Res. 38 (16), 3815–3826.
Oudad, M.A., Kumar, P., Chaali, M., Brar, S.K., Ramirez, A.A., 2022. Optimized ammonium sulphate recovery by stripping-scrubbing sequence system from compost leachate at mesophilic temperatures. Case Stud. Chem. Environ. Eng. 5, 100198 https://doi.org/10.1016/j.cscee.2022.100198.
Palakodeti, A., Azman, S., Rossi, B., Dewil, R., Appels, L., 2021. A critical review of ammonia recovery from anaerobic digestate of organic wastes via stripping. In: Renewable and Sustainable Energy Reviews, 143. Elsevier Ltd.
Pärnamäe, R., Mareev, S., Nikonenko, V., Melnikov, S., Sheldeshov, N., Zabolotskii, V., Hamelers, H.V.M., Tedesco, M., 2021. Bipolar membranes: a review on principles, latest developments, and applications. J. Memb. Sci. 617, 118538 https://doi.org/10.1016/j.memsci.2020.118538.
Petrov, K.V., Mao, M., Santoso, A., Ryzhkov, I.I., Vermaas, D.A., 2023. Design criteria for selective nanofluidic ion-exchange membranes. J. Memb. Sci. 688, 122156.
Qin, Y., Wang, K., Zhou, Z., Yu, S., Wang, L., Xia, Q., Zhao, X., Zhou, C., Ye, J., Wu, Z., 2023. Nitrogen recovery from wastewater as nitrate by coupling mainstream ammonium separation with side stream cyclic up-concentration and targeted conversion. Chem. Eng. J. 455, 140337 https://doi.org/10.1016/j.cej.2022.140337.
Reis, S., Bekunda, M., Howard, C.M., Karanja, N., Winiwarter, W., Yan, X., Bleeker, A., Sutton, M.A., 2016. Synthesis and review: tackling the nitrogen management challenge: from global to local scales. Environ. Res. Lett. 11 (12), 120205.
Rodrigues, M., De Mattos, T.T., Sleutels, T., Ter Heijne, A., Hamelers, H.V.M., Buisman, C.J.N., Kuntke, P., 2020. Minimal bipolar membrane cell configuration for scaling up ammonium recovery. ACS Sustain. Chem. Eng. 8 (47), 17359–17367. https://doi.org/10.1021/acssuschemeng.0c05043.
Rodrigues, M., Molenaar, S., Barbosa, J., Sleutels, T., Hamelers, H.V., Buisman, C.J., Kuntke, P., 2023. Effluent pH correlates with electrochemical nitrogen recovery efficiency at pilot scale operation. Sep. Purif. Technol. 306, 122602.
Ronan, E., Aqeel, H., Wolfaardt, G.M., Liss, S.N., 2021. Recent advancements in the biological treatment of high strength ammonia wastewater. World J. Microbiol. Biotechnol. 37 (9), 158.
Saabas, D., Lee, J., 2022. Recovery of ammonia from simulated membrane contactor effluent using bipolar membrane electrodialysis. J. Memb. Sci. 644, 120081 https://doi.org/10.1016/J.MEMSCI.2021.120081.
Sakar, H., Celik, I., Balcik Canbolat, C., Keskinler, B., Karagunduz, A., 2017. Electrosorption of ammonium by a modified membrane capacitive deionization unit. Sep. Sci. Technol. 52 (16), 2591–2599. https://doi.org/10.1080/01496395.2017.1336556.
Shi, L., Hu, Y., Xie, S., Wu, G., Hu, Z., Zhan, X., 2018. Recovery of nutrients and volatile fatty acids from pig manure hydrolysate using two-stage bipolar membrane electrodialysis. Chem. Eng. J. 334, 134–142. https://doi.org/10.1016/j.cej.2017.10.010.
Shi, L., Xiao, L., Hu, Z., Zhan, X., 2020. Nutrient recovery from animal manure using bipolar membrane electrodialysis: study on product purity and energy efficiency. Water Cycle 1, 54–62. https://doi.org/10.1016/J.WATCYC.2020.06.002.
Soto-Herranz, M., Sánchez-Báscones, M., Antolín-Rodríguez, J.M., Martín-Ramos, P., 2022. Evaluation of different capture solutions for ammonia recovery in suspended gas permeable membrane systems. Membranes 12 (6), 572. https://doi.org/10.3390/membranes12060572.
Starmans, D.A.J., & Melse, R.W. (2011). *Alternatieven voor zwavelzuur in chemische luchtwassers = Alternatives for the use of sulphuric acid in air scrubbers*.
Tanaka, Y., 2015. Chapter six—Electrodialysis. In: Tarleton, S. (Ed.), Progress in Filtration and Separation. Academic Press, pp. 207–284. https://doi.org/10.1016/B978-0-12-384746-1.00006-9.
Ukwuani, A.T., Tao, W., 2016. Developing a vacuum thermal stripping—acid absorption process for ammonia recovery from anaerobic digester effluent. Water Res. 106, 108–115. https://doi.org/10.1016/j.watres.2016.09.054.
van Linden, N., Bandinu, G.L., Vermaas, D.A., Spanjers, H., van Lier, J.B., 2020. Bipolar membrane electrodialysis for energetically competitive ammonium removal and dissolved ammonia production. J. Clean. Prod. 259 https://doi.org/10.1016/j.jclepro.2020.120788.
van Linden, N., Spanjers, H., van Lier, J.B., 2019. Application of dynamic current density for increased concentration factors and reduced energy consumption for concentrating ammonium by electrodialysis. Water Res. 163 https://doi.org/10.1016/j.watres.2019.114856.
van Zelm, R., Seroa da Motta, R.d.P., Lam, W.Y., Menkveld, W., Broeders, E., 2020. Life cycle assessment of side stream removal and recovery of nitrogen from wastewater treatment plants. J. Ind. Ecol. 24 (4), 913–922. https://doi.org/10.1111/jiec.12993.
Vaneeckhaute, C., Claeys, F.H.A., Tack, F.M.G., Meers, E., Belia, E., Vanrolleghem, P.A., 2018. Development, implementation, and validation of a generic nutrient recovery model (NRM) library. Environ. Model. Softw. 99, 170–209. https://doi.org/10.1016/J.ENVSOFT.2017.09.002.
Vaneeckhaute, C., Lebuf, V., Michels, E., Belia, E., Vanrolleghem, P.A., Tack, F.M., Meers, E., 2017. Nutrient recovery from digestate: systematic technology review and product classification. Waste BioMass Valoriz.. 8, 21–40.
Walker, M., Iyer, K., Heaven, S., Banks, C.J., 2011. Ammonia removal in anaerobic digestion by biogas stripping: an evaluation of process alternatives using a first order rate model based on experimental findings. Chem. Eng. J. 178, 138–145. https://doi.org/10.1016/j.cej.2011.10.027.
Ward, A.J., Arola, K., Thompson Brewster, E., Mehta, C.M., Batstone, D.J., 2018. Nutrient recovery from wastewater through pilot scale electrodialysis. Water Res. 135, 57–65. https://doi.org/10.1016/j.watres.2018.02.021.
Wu, H., Vaneeckhaute, C., 2022. Nutrient recovery from wastewater: a review on the integrated Physicochemical technologies of ammonia stripping, adsorption and struvite precipitation. Chem. Eng. J. 433, 133664 https://doi.org/10.1016/j.cej.2021.133664.
Yan, H., Wang, Y., Wu, L., Shehzad, M.A., Jiang, C., Fu, R., Liu, Z., Xu, T., 2019. Multistage-batch electrodialysis to concentrate high-salinity solutions: process optimisation, water transport, and energy consumption. J. Memb. Sci. 570–571, 245–257. https://doi.org/10.1016/j.memsci.2018.10.008.
Yellezuome, D., Zhu, X., Wang, Z., Liu, R., 2022. Mitigation of ammonia inhibition in anaerobic digestion of nitrogen-rich substrates for biogas production by ammonia stripping: a review. Renew. Sustain. Energy Rev. 157, 112043 https://doi.org/10.1016/j.rser.2021.112043.
Zhang, X., Liu, Y., 2021. Circular economy-driven ammonium recovery from municipal wastewater: state of the art, challenges and solutions forward. Bioresour. Technol. 334, 125231.
Zhao, Q.-B., Ma, J., Zeb, I., Yu, L., Chen, S., Zheng, Y.-M., Frear, C., 2015. Ammonia recovery from anaerobic digester effluent through direct aeration. Chem. Eng. J. 279, 31–37. https://doi.org/10.1016/j.cej.2015.04.113.
Zhao, Q., Long, C., Jiang, Z., Yin, W., Tang, A., Yang, H., 2023. Highly stable natural zeolite/montmorillonite hybrid microspheres with green preparation process for efficient adsorption of ammonia nitrogen in wastewater. Appl. Clay. Sci. 243, 106787.
Zhu, S., Kingsbury, R.S., Call, D.F., Coronell, O., 2018. Impact of solution composition on the resistance of ion exchange membranes. J. Memb. Sci. 554, 39–47. https://doi.org/10.1016/j.memsci.2018.02.050.
Zhu, Y., Chang, H., Yan, Z., Liu, C., Liang, Y., Qu, F., Liang, H., Vidic, R.D., 2024. Review of ammonia recovery and removal from wastewater using hydrophobic membrane distillation and membrane contactor. Sep. Purif. Technol. 328, 125094 https://doi.org/10.1016/j.seppur.2023.125094.